March 2002

The surface composition and spin polarization of NiMnSb epitaxial thin films

D. Ristoiu
CNRS Laboratoire Louis Néel, France

J.P. Nozières
CNRS Laboratoire Louis Néel, France

C.N. Borca
University of Nebraska - Lincoln

T. Komesu
University of Nebraska - Lincoln, tkomesu2@unl.edu

H.-K. Jeong
University of Nebraska - Lincoln, hjeong@unl.edu

See next page for additional authors

EUROPHYSICS LETTERS 1 March 2000

Europhys. Lett., **49** (5), pp. 624–630 (2000)

The surface composition and spin polarization of NiMnSb epitaxial thin films

D. Ristoiu[1], J. P. Nozières[1], C. N. Borca[2], T. Komesu[2], H.-k. Jeong[2] and P. A. Dowben[2](*)

[1] *CNRS Laboratoire Louis Néel - 25 avenue des Martyrs BP 166, 38042 Grenoble Cedex 09, France*

[2] *Department of Physics and Astronomy and Center for Materials Research and Analysis Behlen Laboratory of Physics, University of Nebraska-Lincoln Lincoln, NE 68588-0111, USA*

(received 13 September 1999; accepted in final form 15 December 1999)

PACS. 71.20.Lp – Intermetallic compounds.
PACS. 73.20.At – Surface states, band structure, electron density of states.
PACS. 75.25.+z – Spin arrangements in magnetically ordered materials (including neutron and spin-polarized electron studies, synchrotron-source X-ray scattering, etc.).

Abstract. – The composition in the surface region of the Heusler alloy NiMnSb has been studied using angle-resolved X-ray photoemission spectroscopy, low-energy electron diffraction and spin-polarized inverse photoemission. The results are consistent with a generally Mn-Sb terminal layer, though the surface composition is very sensitive to preparation. The surface composition has a critical influence on the polarization near the Fermi level in spin-polarized inverse photoemission. Under some conditions, the polarization at the Fermi level for normal incidence inverse photoemission can reach values very close to 100% above background.

Mn-based Heusler alloys such as NiMnSb and PtMnSb have been predicted to be [1–7] half-metallic ferromagnets (metallic in spin majority and semiconducting in spin minority), *e.g.* fully spin polarized. Unfortunately, experimental evidence of 100% spin polarization near the Fermi level is sadly absent. Using Andreev reflection [8] the spin polarization of NiMnSb was measured to be $58 \pm 2.3\%$, in good agreement with a polarization of about 50% obtained from spin polarized photoemission [9] and consistent with a small perpendicular magnetoresistance for NiMnSb in a spin valve structure [10]. Other bulk measurements have provided evidence of half-metallic character. Indirect measurements using positron annihilation have, however, been interpreted as a proof of full spin polarization at low temperature (10 K) in bulk crystals [11]. A detailed study of the magnetic and transport properties in bulk single crystals has also suggested that NiMnSb is half-metallic at low temperature, with a transition to a metallic state around $T = 80\,\mathrm{K}$ [12]. Two explanations have been put forward to explain the smaller than expected polarization in measurements that are sensitive to electron transport across a surface or interface. The first possibility is that the gap in spin minority is smaller than the expected 0.5 eV [7, 9, 13]. The other possibility is that there is surface segregation [9, 14] making the surface a different material from the bulk. Furthermore, few of these studies on NiMnSb have been undertaken on single crystals or epitaxial thin films.

(*) E-mail: pdowben@unl.edu

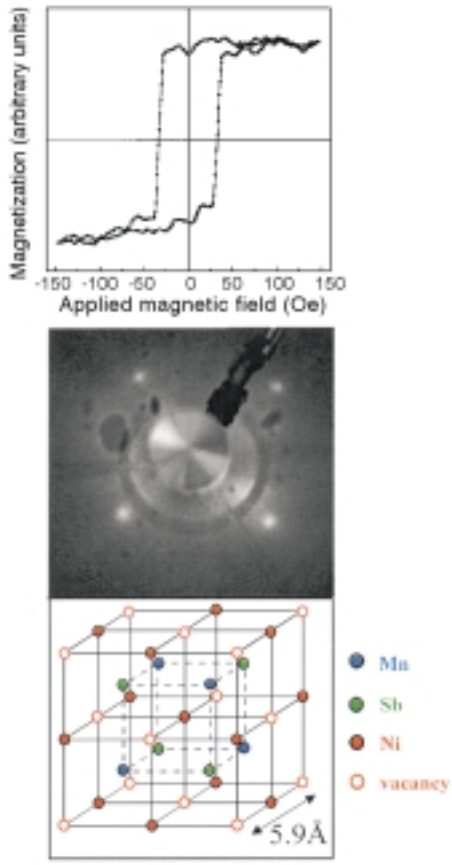

Fig. 1 – The hysteresis loop obtained from magneto-optic Kerr effect of the epitaxial NiMnSb crystalline film along the ⟨110⟩ in-plane direction is shown at top. In the middle, the LEED pattern of a stoichiometric ordered alloy NiMnSb surface obtained through annealing the sample to 700 K. The schematic structure of the cubic NiMnSb lattice is indicated at the bottom ($a = 5.9$ Å).

Because the surface free energy is expected to be different from the bulk, surface segregation is expected in intermetallic compounds. In fact, surface segregation has been routinely observed in some $La_{0.65}A_{0.35}MnO_3$ (A = Ca, Sr, Pb) manganese perovskite oxides [15–17]. An understanding of the influence of surface and interface properties on spin polarization is, therefore, essential if the behavior of half-metallic ferromagnets is to be ever understood in spin tunnel junctions and spin valve structures. This paper explores these surface and interface issues for NiMnSb.

Epitaxial (110)MgO/(100)Mo/(100)NiMnSb thin films were grown by facing targets sputtering. Details of the growth conditions and film structure can be found elsewhere [18]. A 1000 Å Sb capping layer was added to prevent oxidation of the NiMnSb crystalline films. The choice of Sb as the capping layer was dictated by the low temperature for Sb evaporation and because it is a constituent of the Heusler alloy. The Sb capping layers grow epitaxially on NiMnSb with a ⟨100⟩ orientation, a cubic $Pm3m$ structure and a 3.1 Å lattice constant. The crystallinity and orientation of the NiMnSb were established *ex situ* by X-ray diffraction and, once the capping layers were removed, again by low-energy electron diffraction (LEED).

The samples were further characterized by magneto-optic Kerr effect, *ex situ*, to confirm the coercivity of the easy axis, as seen in fig. 1.

The spin-polarized inverse photoemission experiments were undertaken with a transversely polarized spin electron gun based upon the Ciccacci design [19] as described elsewhere [20]. The spin electron gun was designed in a compact form on a separate chamber equipped with an iodine based Geiger-Müller isochromat photon detector with an SrF_2 window. As is typical of such instruments, the electron gun has 28% spin polarization, and the data has been corrected for this incident gun polarization. The direction of electron polarization is in the plane of the sample for all incidence angles, as is the applied field, and spectra were obtained at remanence. The energy resolution was in the vicinity of 400 meV and the wave vector uncertainty is $\pm 0.025\,\text{Å}^{-1}$ for these measurements. The field was applied along the in-plane $\langle 110 \rangle$ easy axis [18] of NiMnSb with magnitudes in excess of 400 Oe, far larger than the samples' saturation and coercive fields of about 40 and 32 Oe, respectively (fig. 1a). The Fermi level was established from tantalum foils in electrical contact with the sample. The core level binding energies and conduction band features are reported with respect to this Fermi level and the emission angle (or incidence angle in the case of the inverse photoemission) is with respect to the surface normal. Typically, several experiments are summed, to improve the signal-to-noise ratio in the spin-polarized inverse photoemission spectra.

Angle-resolved X-ray photoemission spectroscopy (ARXPS) of the Sb, Mn and Ni core levels was undertaken with the Mg-K_α line (1253.6 eV) on a number of different samples. Energy distribution curves of the elemental Ni ($2p_{3/2}$), Mn ($2p_{3/2}$ and $2p_{1/2}$), and Sb ($3d_{5/2}$ and $3d_{3/2}$) core levels were acquired with a large hemispherical electron energy analyzer and the intensities were measured, as were the binding energies, as a function of emission angle, with respect to the surface normal. Intensities are normalized by the cross-section, as measured by Wagner and coworkers [21], with interpolation from the calculations by Scofield for an excitation energy of 1253.6 eV (Mg-K_α) [22] where necessary.

The ARXPS core level data can be utilized to estimate the surface composition of NiMnSb, because the effective mean free path of the escaping electrons becomes shorter with increasing emission angle. The core level intensities can be analyzed using a previously applied semi-empirical method [15, 16, 23] to give a more quantitative picture of the degree of surface segregation. A surface composition can be constructed from comparison of core level intensity ratios for differ elements of the alloy where the measured XPS intensity $I(\theta)$ is normalized by the cross-section (σ_A, σ_B) of the core level of the each element A and B. The normalized intensity ratio is given as

$$R(\theta) = \left[\frac{I_\text{A}(\theta)/\sigma_\text{A}}{I_\text{B}(\theta)/\sigma_\text{B}}\right]\left[\frac{E^p_\text{kin}(\text{A}) - C}{E^p_\text{kin}(\text{B}) - C}\right], \tag{1}$$

where θ is the emission angle with respect to the surface normal, and the term $E^p_\text{kin}(\text{A}) - C$ corrects for the transmission of the electron energy analyzer at the kinetic energy of core level A. Based on the measured transmission functions [24], we have set $p = 0.5$, $C = 0$.

With model calculations utilizing a summation to account for each layer contributing to the photoemission signal, we can understand the angle-resolved XPS data. With the atomic fraction of component A at the j-th layer written as $f_j(\text{A})$, the normalized intensity ratio can be rewritten as

$$R(\theta) = \frac{\displaystyle\sum_{j=0}^{\infty} f_j(\text{A}) e^{jd/\{\lambda_\text{A}\cos(\theta)\}}}{\displaystyle\sum_{j=0}^{\infty} f_j(\text{B}) e^{-jd/\{\lambda_\text{B}\cos(\theta)\}}}, \tag{2}$$

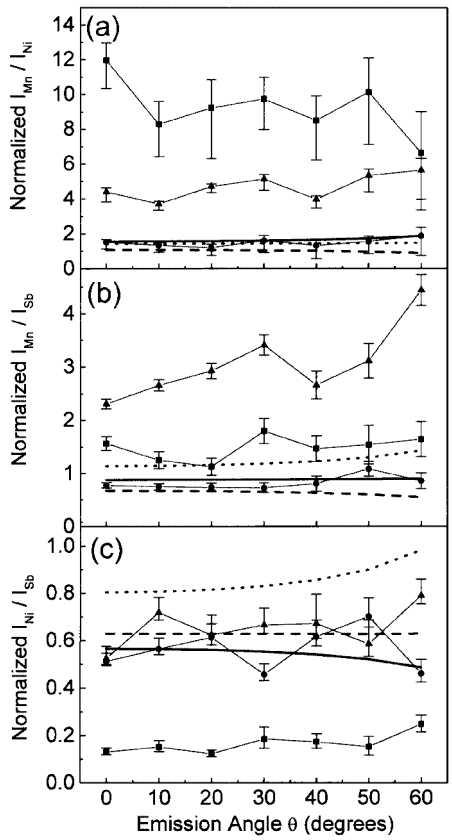

Fig. 2 – Angle-resolved X-ray photoemission intensity ratios of the Ni $2p_{3/2}$, Mn $2p_{3/2} + 2p_{1/2}$, and Sb $3d_{5/2} + 3d_{3/2}$ core levels of NiMnSb after sputter and annealing treatments at 450 K (■), following removal of the excess Sb with a 700 K flash anneal (•) and continued sputtering and annealing cycles (▲). The data are compared to several models for the surface termination including the stoichiometric alloy MnSb(surface) : Ni : $(\mathrm{MnSb} : \mathrm{Ni})_n$ (_____); NiMn(surface) : MnSb : $(\mathrm{Ni} : \mathrm{MnSb})_n$ (———); and NiSb(surface) : MnSb : $(\mathrm{Ni} : \mathrm{MnSb})_n$ (. . . . .).

where λ_{Ni} (7 Å for the Ni $2p_{3/2}$ core), λ_{Mn} (9.35 Å for the Mn $2p$ cores) and λ_{Sb} (10.8 Å for the Sb $3d$ cores) are the effective mean free paths, adapted from the calculated mean free paths of Penn [25]. The NiMnSb crystal structure, summarized by the schematic diagram in fig. 1, is a layered structure with alternate Mn-Sb and Ni-vacancy layers, with a distance between layers approximately $d = a_{\mathrm{NiMnSb}}/4 = 1.5\,\text{Å}$. As the various models for surface termination, considered below, assume no segregation $f_j(\mathrm{A}) = 1/2$ (since we have two elements per layer) or zero depending upon the layer considered.

Sample surfaces were first cleaned in ultra-high vacuum by repeated Ar^+ sputtering and annealing to 450 K. With sufficient sputtering and annealing cycles, the surface was found to be free of both oxygen and carbon, and the LEED pattern is consistent with the 5.9 Å (here 6.0 ± 0.1 Å) lattice constant of NiMnSb. The surface, however, remained antimony rich as is indicated by the low Mn/Sb and particularly Ni/Sb intensity ratios (fig. 2). The latter ratio, in particular, fits with no model for the surface that excludes Sb and Mn segregation or an Sb overlayer with Mn segregation. This antimony-rich surface exhibits virtually no

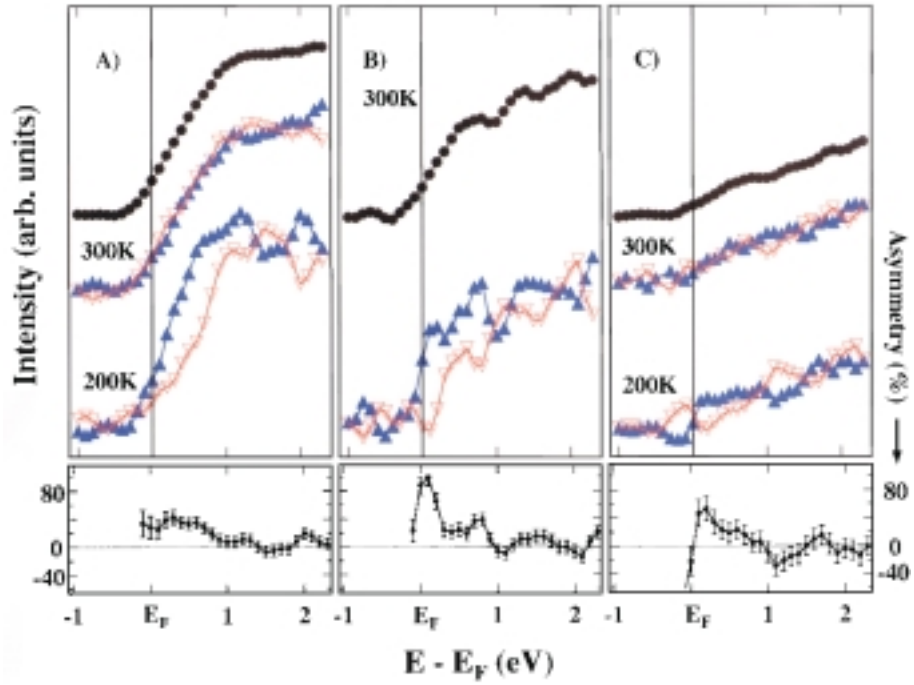

Fig. 3 – Spin-polarized inverse photoemission spectra at normal incidence to NiMnSb (100) with spin-integrated inverse photoemission shown for comparison (•). (a) Following successive sputter and anneal treatments (500 K) and evidence of surface order from LEED. (b) Following the removal of excess Sb through annealing to 700 K and evidence of surface order from LEED. (c) Following additional sputter and anneal treatments after (b). Up triangles (△) indicate spin majority while filled down triangles (▼) indicate spin minority. Below is the polarization asymmetry, above background, shown for the spectra at 200 K (a), 300 K (b) and 200 K (c), respectively, in each panel.

net polarization in spin-polarized inverse photoemission at room temperature but, as the temperature of the sample is decreased to 200 K, the polarization increases to about 30%, or $38 \pm 15\%$ polarization above background (fig. 3a).

We have found that a flash anneal to 700 K removes the excess Sb. The resulting surface is relatively unreactive (a low sticking coefficient for contaminants) and exhibits a sharp LEED pattern, with a 6.0 ± 0.1 Å surface lattice constant (fig. 1b). From the comparison of the ratio of core level intensities for this surface, we find that models that have the surface terminate in NiSb or NiMn do not fit the data nearly as well as the model based upon the stoichiometric alloy terminating in MnSb at the surface, as shown in fig. 2. This near stoichiometric surface may suffer from some Ni depletion in the near surface region, judging from the Mn/Ni and Ni/Sb ratios. Note that annealing of this surface will result in Mn segregation, indicating that the surface free energy differs from that of the bulk, as discussed elsewhere [26].

The stoichiometric or near stoichiometric ordered alloy surface, terminating in MnSb, exhibits very high polarization at the Fermi level in normal-incidence spin-polarized inverse photoemission as seen in fig. 3b. The polarization at the Fermi level is $67 \pm 9\%$ or nearly 100% ($100 + 0/-12\%$) above background. This is significantly higher than the polarization asymmetry of 50%, at room temperature, measured from a polycrystalline sample using spin-polarized photoemission [9], even when the background is included. For these previously

reported spin-polarized photoemission measurements, Sb segregation was observed, which would tend to lower the polarization, as we have just noted.

The data taken at 300 K here from the near stoichiometric ordered alloy surface indicate a conduction band edge, in spin minority, at about 250 meV above the Fermi level. According to calculations for NiMnSb [3], the Fermi level intersects the center of the gap (or slightly above center), in spin minority. Thus these spin-polarized data (at the surface Brillouin zone center or $\boldsymbol{k}_{\parallel} = 0$) are consistent with both a calculated gap in spin minority of about 0.5 eV and a half-metallic system. The data are not, however, conclusive proof that NiMnSb is indeed a half-metallic system. Such a definitive statement would require mapping data at $\boldsymbol{k}$-space points across the Brillouin zone, particularly in the vicinity of the spin majority Fermi level crossings. Nonetheless, this Heusler alloy surface is seen to have far less surface segregation than the manganese perovskites generally [15–17], and exhibits far better surface order than the $La_{0.7}Sr_{0.3}MnO_3$, where a claim of half-metallic character has been made based on the spin-polarized photoemission data [14].

Following the flash anneal to remove the excess Sb at the surface, further sputtering and annealing of NiMnSb samples leads to a degradation of surface order, as seen in the LEED patterns. Changes in the surface composition with continued sputtering and annealing, as indicated by the angle-resolved X-ray photoemission (fig. 2), include Mn segregation but suggest that the Ni/Sb ratio is preserved. These changes in the surface composition are relatively minor (compared to, say, the manganese perovskites [15–17]), but the changes to the unoccupied electronic structure are significant. In all the sample studied, once the excess Sb is removed, the continued sputter and annealing treatments result in a loss of density of state at the Fermi level in inverse photoemission. A drop in the polarization asymmetry, for the unoccupied bands, occurs with continued sputter anneal cycles, as seen in fig. 3c. In the unoccupied band structure, at lower temperatures, there is spin minority at and just below the Fermi level which does not occur with the previous sample surface preparation procedures. This is more reminiscent of MnSb [27] or an antiferromagnetically Mn-rich surface coupled surface layer than the expected electronic structure for NiMnSb.

Clearly the surface of NiMnSb (100) is very fragile and surface preparation and composition have a significant impact on the observed electronic structure. The standard sputter and annealing treatments, used to clean most metal surfaces, lead to Mn segregation in the case of NiMnSb. Very high temperature annealing treatments, to remove surface contamination and restore surface order, would also clearly result in Mn segregation to the surface region. For well-prepared near stoichiometric ordered alloy surfaces, the surface appears to terminate in MnSb and exhibits a high polarization asymmetry at room temperature. The inferred gap in the spin minority sub-band (0.5 eV) is in good agreement with the value expected from band structure calculations. Given the very high sensitivity of the unoccupied electronic structure in inverse photoemission to surface preparation and defects, we cannot be certain that the polarization asymmetry observed here is representative of the bulk electronic structure. Surface states or surface resonances contributions to our data cannot be excluded.

* * *

This work was supported by NSF through grant No. DMR-98-02126, the Center for Materials Research and Analysis (CMRA) and the Nebraska Research Initiative at the University of Nebraska, and the Region Rhone-Alpes through the "Nanotechnologie" program under contract No. PR97024. The authors would like to thank M. Chipara for his assistance with the MOKE measurements.

REFERENCES

[1] de Groot R. A., Mueller F. M., van Engen P. G. and Buschow K. H. J., *Phys. Rev. Lett.*, **50** (1983) 2024.
[2] Wijngaad J. H., Haas C. and de Groot R. A., *Phys. Rev. B*, **40** (1989) 9318.
[3] de Groot R. A., Mueller F. M., van Engen P. G. and Buschow K. H. J., *J. Appl. Phys.*, **55** (1984) 2151; de Groot R. A. and Buschow K. H. J., *J. Magn. & Magn. Mater.*, **43** (1984) 249.
[4] van Engen P. G., Buschow K. H. J., Jongebreur R. and Erman M., *Appl. Phys. Lett.*, **42** (1983) 202.
[5] Kulatov E. and Mazin I. I., *J. Phys. Condens. Matter*, **2** (1990) 343.
[6] Kübler J., Williams A. R. and Sommers C. B., *Phys. Rev. B*, **28** (1983) 1745.
[7] Kang J.-S., Park J.-G., Olson C. G., Youn S. J. and Min B. I., *J. Phys. Condens. Matter*, **7** (1995) 3789.
[8] Soulen R. J. *et al.*, *Science*, **282** (1998) 85.
[9] Bona G. L., Meier F., Taborelli M., Bucher E. and Schmidt P. H., *Solid State Commun.*, **56** (1985) 391.
[10] Caballero J. A., Reilly A. C., Hao Y., Bass J., Pratt W. P., Petroff F. and Childress J. R., *J. Magn. & Magn. Mater.*, **198-199** (1999) 55.
[11] Hanssen K. E. H. M., Mijnarends P. E., Rabou L. P. L. M. and Buschow K. H. J., *Phys. Rev. B*, **42** (1990) 1533.
[12] Hordequin C., Pierre J. and Currat R., *J. Magn. & Magn. Mater.*, **192** (1996) 75.
[13] Kang J.-S., Hong J. H., Jung S. W., Lee Y. P., Park J.-G., Olson C. G., Youn S. J. and Min B. I., *Solid State Commun.*, **88** (1993) 653.
[14] Park J.-H., Vescovo E., Kim H.-J., Kwon C., Ramesh R. and Venkatesan T., *Nature*, **392** (1998) 794.
[15] Jaewu Choi, Waldfried C., Liou S.-H. and Dowben P. A., *J. Vac. Sci. Technol. A*, **16** (1998) 2950.
[16] Jaewu Choi, Jiandi Zhang, Liou S.-H., Dowben P. A. and Plummer E. W., *Phys. Rev. B*, **59** (1999) 13453.
[17] Wei Zhang, Xiaoru Wang and Boyd I., *Appl. Phys. Lett.*, **73** (1998) 2745.
[18] Ristoiu D., Nozières J.-P. and Ranno L., submitted to *J. Magn. & Magn. Mater.*
[19] Ciccaci F., Drouhin H.-J., Hermann C., Houdré R. and Lampel G., *Appl. Phys. Lett.*, **54** (1989) 632.
[20] Waldfried C., McAvoy T., Welipitiya D., Takashi Komesu, Dowben P. A. and Vescovo E., *Phys. Rev. B*, **58** (1998) 7434.
[21] Wagner C. D., Davis L. E., Zeller M. V., Taylor J. A., Raymond R. H. and Gale L. H., *Surf. Interface Anal.*, **3** (1981) 211.
[22] Scofield J. H., *J. Electron. Spectrosc. Relat. Phenom.*, **8** (1976) 129.
[23] Dowben P. A. and Miller A. (Editors), *Core Level Spectroscopy and the Characterization of Surface Segregation* in *Surface Segregation Phenomena* (CRC Press, Boston) 1990, p. 145.
[24] Seah M. P., Jones M. E. and Anthony M. T., *Surf. Interface Anal.*, **6** (1984) 242; Seah M. P., *Surf. Interface Anal.*, **20** (1993) 243.
[25] Penn D. R., *J. Electron. Spectrosc. Relat. Phenom.*, **9** (1976) 29.
[26] Ristoiu D., Borca C. N., Nozières J. P. and Dowben P. A., in preparation.
[27] Coehoorn R., Haas C. and de Groot R. A., *Phys. Rev. B*, **31** (1985) 1980; Okuda H., Senba S., Sato H., Shimada K., Namatame H. and Taniguchi M., *J. Electron. Spectrosc. Relat. Phenom.*, **101-103** (1999) 657; Ravidran P., Delin A., James P., Johansson B., Wills J. M., Ahuja R. and Eriksson O., *Phys. Rev. B*, **59** (1999) 15680; Rader O. *et al.*, *Phys. Rev. B*, **57** (1998) R689.